Int. J. Solids Structures Vol. 27, No. 6, pp. 725–750, 1991
Printed in Great Britain.

0020–7683/91 $3.00 + .00

SURFACE CRACK IN A PLATE UNDER ANTISYMMETRIC LOADING CONDITIONS

P. F. JOSEPH and F. ERDOGAN
Department of Mechanical Engineering and Mechanics, Lehigh University, Bethlehem, PA 18015, U.S.A.

(*Received* 22 *January* 1988; *in revised form* 14 *February* 1990)

Abstract—In this paper the problem of an elastic plate containing a planar surface crack and subjected to antisymmetric loading conditions is considered. The problem is formulated by using Reissner's plate theory. A line spring model is developed for a part-through crack under mixed mode conditions and mode II and III compliance functions are determined. A modification of the integral equations resulting from the Reissner theory is necessary for this formulation to recover the plane strain solution for thin plates. It is shown that, as in three-dimensional problems, mode II and III deformations remain coupled whereas mode I can be separated. The problem is solved and mode II and III stress intensity factors are given for a plate containing a surface crack which is subjected to three separate antisymmetric external loads, namely in-plane shear, twisting moment, and transverse shear. Results for in-plane shear and transverse shear are compared with existing numerical solutions. The results presented also include the effect of Poisson's ratio.

1. INTRODUCTION

Generally, surface cracks growing under cyclic loading and/or corrosive environment are oriented in such a way that the stress state along the crack front is purely mode I. Largely for this reason and partly because of the complexity of the related analysis, the vast majority of existing solutions of the surface crack problem in a plate are restricted to mode I loading conditions. For the analyst one highly discouraging aspect of the problem is that under mixed mode loading conditions the crack usually does not remain coplanar as it grows. However, it is possible to envision structural components subjected to fully reversed cyclic antisymmetric loading (particularly in the presence of a sustained or cyclic mode I loading of some significant magnitude) in which, because of symmetry, the surface crack may initiate and grow in a planar fashion. Under cyclic torsion for example, despite the local saw-tooth type irregularities, macroscopically the growing crack in shafts is known to remain generally coplanar (Tschegg *et al.*, 1983).

Since in three-dimensional crack problems mode II and III deformations are always coupled, the only fracture mechanics parameter that can logically be used in these problems to correlate the subcritical crack growth results would be the strain energy release rate. Thus, in order to model the subcritical crack growth process and to analyze the results under mixed mode loading conditions, the solution of the corresponding crack problem would be needed. The main interest in this paper is in structural components that can locally be represented by a "plate", contain a planar surface crack, and are subjected to general loading conditions. It is further assumed that the plane of the crack is perpendicular to the plate. Given the general part-through crack problem for a plate, the mode I component can always be separated and treated independently by simply considering the membrane and bending resultants N_{11} and M_{11} as the only applied loads (Fig. 1). In this study, therefore, only the effect of the antisymmetric external loads N_{12}, M_{12} and V_1 resulting in mode II and III deformations around the crack will be considered (Fig. 1).

The surface crack problem shown in Fig. 1 is a three-dimensional problem which does not readily lend itself to analytical treatment. The existing elasticity solutions of the problem have, therefore, been based largely on the finite element, boundary element, or alternating methods. Quite understandably the mode I surface crack problem has been studied rather extensively [see the recent review articles by Atluri and Nishioka (1986) and by Newman and Raju (1986) for a nearly complete list of references], whereas there are only a few solutions dealing with the mixed mode problem (Smith and Sorensen, 1974; Simon *et al.*,

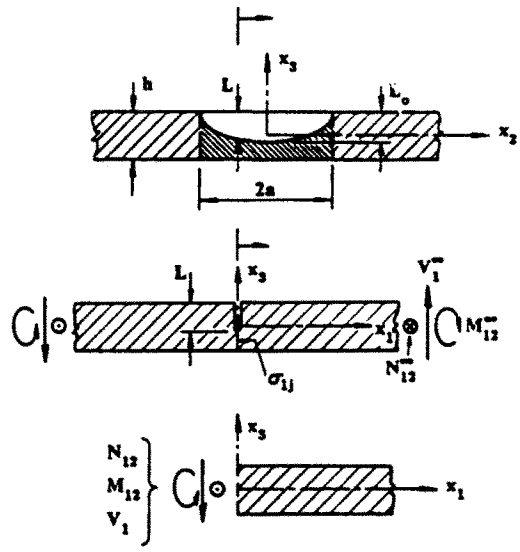

Fig. 1. Notation for a surface crack in a plate under antisymmetric loading.

1987; Nikishkov and Atluri, 1987). The problem can, however, be treated analytically within the confines of a plate theory by approximating the net ligament in the plate by a line spring (Rice and Levy, 1972; see also the review article by Erdogan, 1986, for references). Most of the studies that are based on the line spring model deal with the surface crack problem under mode I loading conditions only. Li and Rice (1983) were the first to apply the line spring principle to the antisymmetric surface crack problem. Their model was a simplified version of the mode I model; it applied only to long cracks and made use of the classical plate theory which cannot properly handle twisting and transverse shear separately. Later, Desvaux (1985) applied the line spring idea to a plate that was modeled by the finite element package ABAQUS which can include transverse shear deformation. In his work he found a problem with the twisting component of the model. Among other difficulties the model, without some correction, will not recover the plane strain solution for long cracks. This behavior should be an inherent part of the model. To overcome this problem they ignored the line spring compliance coefficient that causes coupling between in-plane shear and twisting moment. This coefficient is analogous to the mode I coefficient which couples tension to bending. We believe it should remain in the line spring equations. This assumption leads to inaccurate stress intensity factors as compared to the solutions given by Sorensen and Smith (1977) for the most important antisymmetric loading condition of in-plane shear. In this paper the line spring model will be developed for a plate containing a surface crack and subjected to antisymmetric external loads. The model is then adjusted such that the plane strain solution will be predicted for long cracks. The mode II and III stress intensity factors will then be computed for various loading conditions. Comparisons with existing solutions will be made.

2. LINE SPRING MODEL FOR ANTISYMMETRIC DEFORMATIONS

Consider a plate containing a through crack of length $2a$ which is subjected to antisymmetric applied loads having the resultants N_{12}, M_{12} and V_1 (Fig. 1). Assume that the plate problem for the given applied loads has been solved in the absence of the crack and that the problem is thus reduced to a perturbation problem in which the crack surface tractions are the only non-zero external loads. Let u_1, u_2 and u_3 be the components of the displacement vector and β_1 and β_2 those of the rotation on the neutral plane $x_3 = 0$ (Fig. 1). Define the antisymmetric complementary "stress" and "displacement" quantities on the line $x_1 = 0, x_3 = 0, -\infty < x_2 < \infty$ by (Fig. 1)

$$N_{12}(0,x_2)=F_1(x_2),\quad M_{12}(0,x_2)=F_2(x_2),\quad V_1(0,x_2)=F_3(x_2), \tag{1}$$

$$u_2(+0,x_2)=g_1(x_2),\quad \beta_2(+0,x_2)=g_2(x_2),\quad u_3(+0,x_2)=g_3(x_2). \tag{2}$$

By using the displacements as the unknown functions and Reissner's transverse shear theory in the formulation of plate bending (Reissner, 1945, 1947) for the through crack, the integral equations may be obtained as follows [see Kaya and Erdogan (1987) for the discussion of integral equations with strongly singular kernels and Joseph and Erdogan (1987) for the details of the derivations]:

$$\frac{1}{2\pi}\int\!\!\!\!\!\!-_{-a}^{a}\frac{g_1(t_2)}{(t_2-x_2)^2}\,dt_2=\frac{1}{Eh}F_{10}(x_2),\quad -a<x_2<a, \tag{3}$$

$$\frac{h}{24\pi}\int\!\!\!\!\!\!-_{-a}^{a}\frac{g_2(t_2)}{(t_2-x_2)^2}\,dt_2+\frac{1}{2\pi}\int_{-a}^{a}\sum_{j=2}^{3}k_{2j}(z)g_j(t_2)\,dt_2=\frac{1}{Eh^2}F_{20}(x_2),\quad -a<x_2<a, \tag{4}$$

$$\frac{1}{\pi}\int\!\!\!\!\!\!-_{-a}^{a}\frac{g_3(t_2)}{(t_2-x_2)^2}\,dt_2+\frac{1}{2\pi}\int_{-a}^{a}\sum_{j=2}^{3}k_{3j}(z)g_j(t_2)\,dt_2=\frac{12(1+\nu)}{5Eh}F_{30}(x_2),\quad -a<x_2<a, \tag{5}$$

where F_{i0} $(i=1,2,3)$ are the crack surface tractions that are equal and opposite to the stress resultants obtained from the solution of the uncracked problem [see eqn (1)] and the kernels k_{ij} $(i,j=2,3)$ are given by

$$k_{22}(z)=\frac{5}{12h(1+\nu)}\left[\frac{48}{z^4}-\frac{4}{z^2}+2K_0(|z|)-4K_2(|z|)-\frac{24}{z^2}K_2(|z|)\right],$$

$$k_{23}(z)=\frac{5\sqrt{10}}{12h^2(1+\nu)}\left[\frac{-8}{z^3}-zK_0(|z|)+\left(z+\frac{4}{z}\right)K_2(|z|)\right],$$

$$k_{32}(z)=\frac{\sqrt{10}}{h}\left[\frac{8}{z^3}+zK_0(|z|)-\left(z+\frac{4}{z}\right)K_2(|z|)\right],$$

$$k_{33}(z)=\frac{10}{h^2}\left[K_2(|z|)-\frac{2}{z^2}+K_0(|z|)\right],$$

$$z=\frac{\sqrt{10}}{h}(t_2-x_2). \tag{6a–e}$$

In (6) K_0 and K_2 are the modified Bessel functions of the second kind. For small values of z the kernels k_{ij} $(i,j=2,3)$ have the following asymptotic form:

$$k_{22}(z)\sim\frac{5}{12h(1+\nu)}[\ln(|z|/2)+(\gamma_e-1/4)+(z/2)^2\ln(|z|/2)+\cdots],$$

$$k_{23}(z)\sim\frac{5\sqrt{10}}{12h^2(1+\nu)}[(z/2)\ln(|z|/2)+(z/2)(\gamma_e-1/4)+(2/3)(z/2)^3\ln(|z|/2)+\cdots],$$

$$k_{32}(z)\sim\frac{\sqrt{10}}{h}[-(z/2)\ln(|z|/2)-(z/2)(\gamma_e-1/4)-(2/3)(z/2)^3\ln(|z|/2)+\cdots],$$

$$k_{33}(z)\sim\frac{10}{h^2}[-\ln(|z|/2)-(1/2+\gamma_e)-(3/2)(z/2)^2\ln(|z|/2)+\cdots],$$

$$z=\frac{\sqrt{10}}{h}(t_2-x_2), \tag{7a–e}$$

where $\gamma_e = 0.577215665$ is Euler's constant. From (7) it is seen that the functions k_{ij} $(i, j = 2, 3)$ that appear in (3)–(5) are square integrable in the closed interval $[-a, a]$ and can therefore be treated as Fredholm kernels.

In formulating the three-dimensional surface crack problem shown in Fig. 1 by the "line spring" model, first the problem is rendered two-dimensional by suppression of the x_3 coordinate through the use of a "plate theory". Then the unknown stresses $\sigma_{1j}(0, x_2, x_3)$ $(j = 2, 3)$, along the net ligament $[x_1 = 0, -a < x_2 < a, (-h/2) < x_3 < (h/2 - L)]$ are represented by their statically equivalent resultants $N_{12}(x_2)$, $M_{12}(x_2)$ and $V_1(x_2)$ (Fig. 1). These resultants which act on the crack along the neutral axis $x_1 = 0$, $-a < x_2 < a$, $x_3 = 0$ are assumed to replace the effect of the net ligament and tend to constrain crack surface displacements. Thus, the part-through crack problem may now be formulated approximately by using the through crack formulation given in (3)–(5) under the assumption that the unknown resultants, which are equivalent to $\sigma_{1j}(0, x_2, x_3)$ $(j = 2, 3)$, act as additional external loading. The integral equations of the problem may then be obtained by modifying (3)–(5) as follows:

$$\frac{1}{2\pi}\int_{-a}^{a}\sum_{j=1}^{3}\left[\frac{A_i\delta_{ij}}{(t_2-x_2)^2}+k_{ij}(z)\right]g_j(t_2)\,dt_2 = B_i[F_{i0}(x_2)+F_i(x_2)] \quad (i=1,2,3), \quad (-a<x_2<a), \tag{8}$$

where the constants A_i, B_i $(i = 1, 2, 3)$ are given in (3)–(5), the kernels k_{ij} $(i, j = 1, 2, 3)$ by (6) with $k_{1m} = 0 = k_{m1}$ $(m = 2, 3)$ and F_i $(i = 1, 2, 3)$ are defined by

$$F_1(x_2) = N_{12}(x_2) = \int_{h/2}^{h/2-L}\sigma_{12}(0, x_2, x_3)\,dx_3,$$

$$F_2(x_2) = M_{12}(x_2) = \int_{h/2}^{h/2-L}\sigma_{12}(0, x_2, x_3)x_3\,dx_3,$$

$$F_3(x_2) = V_1(x_2) = \int_{-h/2}^{h/2-L}\sigma_{13}(0, x_2, x_3)\,dx_3. \tag{9a-c}$$

Clearly the net ligament resultants F_1, F_2 and F_3 are not independent of the crack surface displacements and rotations g_1, g_2 and g_3. Thus the formulation of the crack problem is completed by establishing the relationship between F_i and g_i $(i = 1, 2, 3)$. To do this the energy G available for fracture at a location along the crack front is expressed in two different ways, namely as the crack closure energy expressed in terms of the stress intensity factors and as the product of load–load point displacement (Rice and Levy, 1972; Rice, 1972). If U and V respectively refer to the work done by the external loads and the strain energy, for the antisymmetric problem under consideration G can be expressed as

$$\frac{\partial}{\partial L}(U-V) = G = \frac{\pi(1-\nu^2)}{E}\left(k_2^2+\frac{1}{1-\nu}k_3^2\right). \tag{10}$$

where $k_2(x_2)$ and $k_3(x_2)$ are the mode II and III stress intensity factors along the crack front defined by

$$k_2(x_2) = \lim_{r\to 0}\sqrt{2r}\sigma_{13}(0, x_2, x_3),$$

$$k_3(x_2) = \lim_{r\to 0}\sqrt{2r}\sigma_{12}(0, x_2, x_3), \quad r = h/2 - L - x_3. \tag{11a, b}$$

$g_1(t_2$

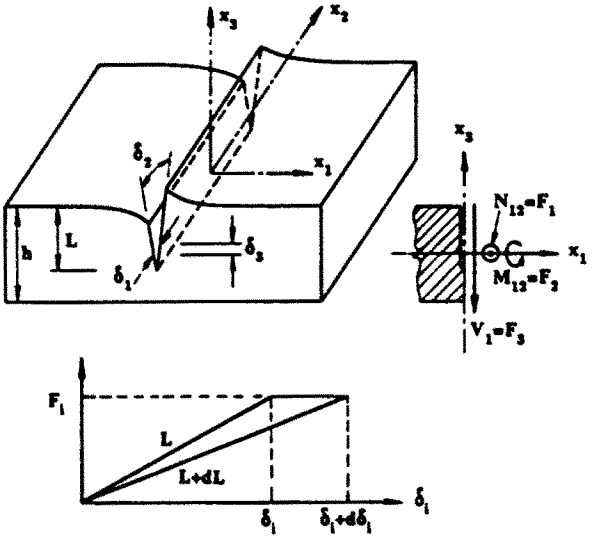

Fig. 2. Notation for a plate with an edge crack under two-dimensional antisymmetric loading.

Referring now to Fig. 2, locally for a change dL in the crack length L, the change in U and V under constant load may be expressed as

$$dU = \sum_{i=1}^{3} F_i \, d\delta_i, \tag{12}$$

$$dV = \sum_{i=1}^{3} \left[\frac{1}{2} F_i(\delta_i + d\delta_i) - \frac{1}{2} F_i \delta_i \right] = \frac{1}{2} \sum_{i=1}^{3} F_i \, d\delta_i, \tag{13}$$

where $d\delta_i$ is the variation in the relative crack surface displacement δ_i (Fig. 2). For the antisymmetric problem considered from (2) it may be seen that

$$\delta_i(x_2) = 2g_i(x_2) \quad (i = 1, 2, 3). \tag{14}$$

From (12) and (13) the incremental energy available for fracture corresponding to crack growth of an amount dL is found to be

$$d(U - V) = \sum_{i=1}^{3} \frac{1}{2} F_i \, d\delta_i. \tag{15}$$

Considering

$$d\delta_i = \frac{\partial \delta_i}{\partial L} dL \quad (i = 1, 2, 3), \tag{16}$$

from (15) and (10) it then follows that

$$\frac{\partial}{\partial L}(U - V) = \sum_{i=1}^{3} \frac{1}{2} F_i \frac{\partial \delta_i}{\partial L} \tag{17}$$

and

$$\sum_{i=1}^{3} \frac{1}{2} F_i \frac{\partial \delta_i}{\partial L} = \frac{\pi(1-\nu^2)}{E}\left(k_2^2 + \frac{1}{1-\nu}k_3^2\right). \tag{18}$$

A further assumption made in developing the line spring model is that the stress intensity factors k_2 and k_3 at a location x_2 along the crack front may be related to the resultants $F_i(x_2)$ $(i = 1, 2, 3)$ through the solution of the plane edge crack problem shown in Fig. 2. Assume that this solution is known and that the stress intensity factors are given by (see the next section)

$$k_2(x_2) = \sqrt{h}\sigma_3(x_2) f_3(\xi),$$
$$k_3(x_2) = \sqrt{h}[\sigma_1(x_2) f_1(\xi) + \sigma_2(x_2) f_2(\xi)], \quad \xi = L(x_2)/h, \tag{19a, b}$$

where the shape functions f_1, f_2 and f_3 are assumed to be known and σ_1, σ_2 and σ_3 are stress amplitudes in the plate defined by (Fig. 2)

$$\sigma_1(x_2) = \frac{1}{h} F_1(x_2),$$
$$\sigma_2(x_2) = \frac{6}{h^2} F_2(x_2),$$
$$\sigma_3(x_2) = \frac{3}{2h} F_3(x_2), \quad -a < x_2 < a. \tag{20a–c}$$

In the plate theory used σ_{12} is linear and σ_{13} is parabolic in the thickness coordinate x_3. From (14) and (18)–(20) it follows that

$$\sigma_1 \frac{\partial g_1}{\partial L} + \frac{h}{6}\sigma_2 \frac{\partial g_2}{\partial L} + \frac{2}{3}\sigma_3 \frac{\partial g_3}{\partial L} = \frac{\pi(1-\nu^2)}{E}\left[\frac{1}{1-\nu}(\sigma_1^2 f_1^2 + 2\sigma_1\sigma_2 f_1 f_2 + \sigma_2^2 f_2^2) + \sigma_3^2 f_3^2\right]. \tag{21}$$

If we now define the matrices

$$\{\sigma\} = \begin{Bmatrix} \sigma_1 \\ \sigma_2 \\ \sigma_3 \end{Bmatrix}, \quad \{g\} = \begin{Bmatrix} g_1 \\ (h/6)g_2 \\ (2/3)g_3 \end{Bmatrix}, \quad [f] = \frac{\pi(1+\nu)}{E}\begin{bmatrix} f_1^2 & f_1 f_2 & 0 \\ f_1 f_2 & f_2^2 & 0 \\ 0 & 0 & (1-\nu) f_3^2 \end{bmatrix}, \tag{22a–c}$$

from (21) it is seen that

$$\{\sigma\}^{\mathrm{T}} \frac{\partial}{\partial L}\{g\} = \{\sigma\}^{\mathrm{T}}[f]\{\sigma\}, \quad \frac{\partial}{\partial L}\{g\} = [f]\{\sigma\}. \tag{23}$$

By observing that σ is independent of $L = h\xi$ and $\{g\} = 0$ for $L = 0$, (23) may be integrated to give

$$\{g(x_2)\} = h\left(\int_0^{\xi} [f(\xi)]\, d\xi\right)\{\sigma(x_2)\}, \quad \xi = L(x_2)/h. \tag{24}$$

In terms of the known functions f_i $(i = 1, 2, 3)$, if we define

$$\alpha_{ij} = \int_0^{\xi} f_i f_j \, d\xi \quad (i, j = 1, 2),$$

$$\alpha_{33} = (1-\nu)\int_0^{\xi} f_3 f_3 \, d\xi, \quad \alpha_{i3} = \alpha_{3i} = 0 \quad (i = 1, 2), \tag{25}$$

$$[A] = [\alpha_{ij}] \quad (i, j = 1, 2, 3), \tag{26}$$

from (22) and (24) we find

$$\{g(x_2)\} = \frac{\pi h(1+\nu)}{E}[A]\{\sigma(x_2)\}, \tag{27}$$

$$\{\sigma(x_2)\} = \frac{E}{\pi h(1+\nu)}[A]^{-1}\{g(x_2)\}. \tag{28}$$

With (20) and (22b), (28) gives the desired relationship between F_i and g_i ($i = 1, 2, 3$), and (8) becomes a system of integral equations in $g_i(x_2)$. Specifically, from (28) we obtain

$$\sigma_1 = \frac{E}{\pi h(1+\nu)}\left(\gamma_{11} g_1 + \frac{h}{6}\gamma_{12} g_2\right),$$

$$\sigma_2 = \frac{E}{\pi h(1+\nu)}\left(\gamma_{21} g_1 + \frac{h}{6}\gamma_{22} g_2\right),$$

$$\sigma_3 = \frac{E}{\pi h(1+\nu)}\gamma_{33}\frac{2}{3} g_3, \tag{29a-c}$$

where

$$\gamma_{11} = \frac{\alpha_{22}}{\Delta}, \quad \gamma_{12} = \gamma_{21} = \frac{-\alpha_{12}}{\Delta}, \quad \gamma_{22} = \frac{\alpha_{11}}{\Delta},$$

$$\gamma_{33} = \frac{1}{\alpha_{33}}, \quad \Delta = \alpha_{11}\alpha_{22} - \alpha_{12}^2. \tag{30}$$

By substituting (20) and (29) into (8), the system of integral equations becomes

$$\frac{1}{2\pi}\fint_{-a}^{a} \frac{g_1(t_2)}{(t_2 - x_2)^2} dt_2 - \frac{1}{\pi h(1+\nu)}\left(\gamma_{11}(x_2) g_1(x_2) + \frac{h}{6}\gamma_{12}(x_2) g_2(x_2)\right) = \frac{1}{Eh} F_{10}(x_2), \quad -a < x_2 < a, \tag{31}$$

$$\frac{h}{24\pi}\fint_{-a}^{a} \frac{g_2(t_2)}{(t_2 - x_2)^2} dt_2 + \frac{1}{2\pi}\int_{-a}^{a} \sum_{j=2}^{3} k_{2j}(z) g_j(t_2) \, dt_2 - \frac{1}{6\pi h(1+\nu)}\left(\gamma_{21}(x_2) g_1(x_2) + \frac{h}{6}\gamma_{22}(x_{22}) g_2(x_2)\right) = \frac{1}{Eh^2} F_{20}(x_2), \quad -a < x_2 < a, \tag{32}$$

$$\frac{1}{\pi}\int_{-a}^{a}\frac{g_3(t_2)}{(t_2-x_2)^2}dt_2+\frac{1}{2\pi}\int_{-a}^{a}\sum_{j=2}^{3}k_{3j}(z)g_j(t_2)\,dt_2$$

$$-\frac{16}{15\pi h}\gamma_{33}(x_2)g_3(x_2)=\frac{12(1+\nu)}{5Eh}F_{30}(x_2),\quad -a<x_2<a. \tag{33}$$

After solving the integral equations (31)–(33) for g_i ($i=1, 2, 3$), the stress amplitudes $\sigma_i(x_2)$ ($i=1, 2, 3$) at a location x_2 ($-a<x_2<a$) may be obtained from (29). The stress intensity factors $k_2(x_2)$ and $k_3(x_2)$ along the crack front may then be evaluated from (19).

From (11) it is seen that in developing the line spring model the stress intensity factors $k_2(x_2)$ and $k_3(x_2)$ are defined in terms of the stress components σ_{13} and σ_{12}, respectively (Fig. 1). The conventional concept of mode II and III stress intensity factors requires that they be defined in terms of stresses referred to a coordinate system that consists of the normal and the tangent to the crack boundary and the normal to the crack plane. Thus, if we let x_2' and x_3' be the tangent and the normal to the crack front in the x_2x_3 plane (Fig. 1) and θ be the angle between the x_2 and x_2' axes, transforming the stress tensor to x_1', x_2', x_3' coordinates the mode II and III stress intensity factors may be expressed as

$$k_2'=-k_3\sin\theta+k_2\cos\theta,$$
$$k_3'=k_3\cos\theta+k_2\sin\theta, \tag{34a, b}$$

where for the typical case of a semi-elliptic profile, the angle θ is given by

$$\theta=\tan^{-1}\left(\frac{(L_0/a)(x_2/a)}{\sqrt{1-(x_2/a)^2}}\right). \tag{35}$$

Note that such a rotation will not affect the mode I result.

When the preceding formulation is used it becomes apparent that there is a problem for large values of the normalized half crack length a/h. As $a/h\to\infty$, the plane strain solution is not recovered. Because of the underlying assumptions made, this large a/h behavior of the solution should be an inherent part of the model. In terms of the plate variables, the plane strain limit is represented by the following algebraic equations that can be solved in terms of the known loads, $F_{i0}(x_2)$ ($i=1, 2, 3$):

$$\frac{\sigma_1(x_2)}{E}=\frac{1}{Eh}F_{10}(x_2)=\frac{-1}{\pi h(1+\nu)}\left(\gamma_{11}(x_2)g_1(x_2)+\frac{h}{6}\gamma_{12}(x_2)g_2(x_2)\right),$$

$$\frac{\sigma_2(x_2)}{6E}=\frac{1}{Eh^2}F_{20}(x_2)=\frac{-1}{6\pi h(1+\nu)}\left(\gamma_{21}(x_2)g_1(x_2)+\frac{h}{6}\gamma_{22}(x_2)g_2(x_2)\right)$$

$$\frac{8(1+\nu)\sigma_3(x_2)}{5Eh}=\frac{12(1+\nu)}{5Eh}F_{30}(x_2)=\frac{-16}{15\pi h}\gamma_{33}(x_2)g_3(x_2),\quad -a<x_2<a. \tag{36a–c}$$

By comparing these equations with the integral equations (31)–(33), it is clear that the integrated terms of (31)–(33) should collectively drop out as $a/h\to\infty$. In the mode I formulation the integrated terms individually vanish for $a/h\to\infty$ and the plane strain case is properly recovered.

At this point it is worthwhile examining how this limit is obtained for the mode I case. This will hopefully show why the antisymmetric formulation fails to recover this result.

First we consider the through crack equations for tension and bending (see, for example, Joseph and Erdogan, 1989). The equation for tension is identical to the in-plane shear equation (3). The bending equation is similar to the equation for twisting (4) as shown below:

$$\frac{h}{24\pi}\int_{-a}^{a}\frac{\beta_1(t_2)}{(t_2-x_2)^2}\,dt_2+\frac{1}{2\pi}\int_{-a}^{a}k_{bb}(z)\beta_1(t_2)\,dt_2=\frac{-\sigma_b}{6E},\quad -a<x_2<a, \tag{37}$$

where

$$k_{bb}(z)=-k_{22}(z)-\frac{5}{12h(1+\nu)}2K_0(|z|). \tag{38}$$

The right-hand sides of these uncoupled equations are σ_t/E for tension and $\sigma_b/6E$ for bending. If we assume these ratios to be of order one, then for proper balancing of terms in the equation, the sum of the integral terms must also be of order one for $-a<x_2<a$. This is true for all h/a. Given the kernels in the mode I problem, this balancing is accomplished by having the displacement v, which corresponds to tension, proportional to the half crack length a, and the rotation β_1, which corresponds to bending, proportional to a/h.

If we now consider the integral equations for the part-through crack, the above result is no longer valid. The scaling changes with the addition of the line spring terms. These terms are dominant, and must therefore balance with the right-hand sides of the equations which are the same as for the through crack case. Now the displacement quantity v is proportional to h, and β_1 is independent of both a and h. Note that this result simply comes from the plane edge crack problem which is independent of a. The effect of this scaling on the integral terms is to force them to be of order h/a. Therefore, as $h/a\to 0$ the integral terms drop out and the plane strain equations, analogous to (36a–c), are recovered for the mode I case.

Now it is perhaps necessary to give a physical interpretation of what has just been said. First, the physical interpretation of an infinite displacement, particularly an infinite rotation, is simply that an infinitely thin plate with a through crack has no resistance to finite loading. This resistance could have come from the stiffness of the local plate edge and/or the clamping effect of the distant crack ends. The physical reasoning as to why the integral terms in the part-through crack case approach zero as $h/a\to 0$, is that neither one of these factors can prevent the crack surfaces from displacing or rotating (note that all the terms in the integral equations represent force quantities). The local stiffness of the plate edge becomes negligible and the mechanics of the problem away from the crack ends is not affected by the crack ends. In the part-through crack problem, the only remaining means of resistance comes from the net ligament forces which are represented by the line spring terms. These terms come from the solution of an elasticity problem and properly account for any local "stiffness" that the plate may have. The problem is now identical to the line spring model version of the plane edge crack problem, and therefore the plane strain solution is recovered.

In the antisymmetric case one would expect the same behavior. The infinitely thin plate with a through crack should not support finite in-plane shear, transverse shear or twisting loading. The corresponding displacements would then become infinite for $h/a\to 0$. If this were the case, then as in the mode I line spring model, all integral terms would vanish, and the plane strain equations (36a–c) would result. However, this does not happen because the local twisting stiffness of the plate does not diminish as $h/a\to 0$. As mentioned in the previous paragraph, for the line spring model to work, the line spring terms should account for all local plate stiffness as $h/a\to 0$.

The problem from a mathematical point of view is that the twisting kernels, both k_{22} and k_{23} in (4), do not reduce the magnitude of their corresponding displacement as $h/a\to 0$. An order one value of the displacements $g_2(x_2)$ and $g_3(x_2)$, after being integrated with

k_{22} and k_{23} respectively, will result in an order one term. These integral terms are therefore of the same order of magnitude as the line spring terms for small h/a. This prevents the plane strain solution from being reached.

First we examine the small h/a behavior of the twisting kernels. As will now be shown, these kernels behave like delta functions for $h/a \to 0$. First note that for $a/h \to \infty$ (or $h \to 0$), from (6a) and (6e) $k_{22}(z) \to 0$ except at $t_2 = x_2$ where $k_{22}(z)$ is infinite, as seen from (7a). A delta function must also have the property that its integral from negative infinity to positive infinity be finite and non-zero. By rewriting (6a) as follows:

$$k_{22}(z) = \frac{5}{12h(1+\nu)}\left[-2K_0(z) - \frac{\mathrm{d}}{\mathrm{d}z}\left(\frac{16}{z^3} - \frac{4}{z} - \frac{8}{z}K_2(z)\right)\right], \tag{39}$$

it is easy to show that

$$\lim_{a/h\to\infty} \frac{1}{2\pi}\int_{-a}^{a} k_{22}(z)\,\mathrm{d}t_2 = \frac{-\sqrt{10}}{24\pi(1+\nu)}\int_{-\infty}^{\infty} K_0(|z|)\,\mathrm{d}z = \frac{-\sqrt{10}}{24(1+\nu)}, \tag{40}$$

where the following result has been used:

$$\int_0^{\infty} K_0(z)\,\mathrm{d}z = \frac{\pi}{2}. \tag{41}$$

Therefore we have

$$\lim_{a/h\to\infty} \frac{1}{2\pi}\int_{-a}^{a} k_{22}(z)g_2(t_2)\,\mathrm{d}t_2 = \frac{-\sqrt{10}}{24(1+\nu)}\int_{-\infty}^{\infty} \delta(x_2-t_2)g_2(t_2)\,\mathrm{d}t_2 = \frac{-\sqrt{10}}{24(1+\nu)}g_2(x_2). \tag{42}$$

In a similar way, by using the following equivalent form of (6b),

$$k_{23}(z) = \frac{5\sqrt{10}}{12h^2(1+\nu)}\frac{\mathrm{d}}{\mathrm{d}z}\left[\frac{\mathrm{d}}{\mathrm{d}z}\left(\frac{-2}{z} - 2z[K_0(z)-K_2(z)]\right) + 2K_0(z)\right], \tag{43}$$

it may be shown that

$$\lim_{a/h\to\infty} \frac{1}{2\pi}\int_{-a}^{a} k_{23}(z)g_3(t_2)\,\mathrm{d}t_2 = \frac{-\sqrt{10}}{24(1+\nu)}\frac{\mathrm{d}g_3(x_2)}{\mathrm{d}x_2}. \tag{44}$$

For these two cases, the integral term will be of order one if the displacement is of order one. All other integrated terms of (31)–(33) vanish individually as a/h becomes large. Therefore the limit of (31)–(33) is not as given by (36a–c) but rather by the following set of equations:

$$\frac{1}{Eh}F_{10}(x_2) = \frac{-1}{\pi h(1+\nu)}\left(\gamma_{11}(x_2)g_1(x_2) + \frac{h}{6}\gamma_{12}(x_2)g_2(x_2)\right),$$

$$\frac{1}{Eh^2}F_{20}(x_2) = \frac{-1}{6\pi h(1+\nu)}\left(\gamma_{21}(x_2)g_1(x_2) + \frac{h}{6}\gamma_{22}(x_2)g_2(x_2)\right) + \frac{-\sqrt{10}}{24(1+\nu)}\left(g_2(x_2) + \frac{\mathrm{d}g_3(x_2)}{\mathrm{d}x_2}\right),$$

$$\frac{12(1+\nu)}{5Eh}F_{30}(x_2) = \frac{-16}{15\pi h}\gamma_{33}(x_2)g_3(x_2). \tag{45a–c}$$

It should be pointed out that the term resulting from k_{23} is much smaller than that from k_{22} for large a/h. In the part-through crack problem, as h/a approaches zero, the transverse displacement $g_3(x_2)$ approaches either a constant value for transverse shear loading or zero for twisting or in-plane shear loading. It follows that the derivative of $g_3(x_2)$ as given by (44) approaches zero for large a/h. Therefore, the mathematical reason why this formulation does not recover the plane strain result is the presence of the term given by (42). Note that this delta function term is similar to the line spring terms and effectively changes γ_{22} in (45b). In this thesis, Desvaux (1985) remarked that the twisting moment was working too hard. This delta function term is the reason why.

In order to understand the consequences of this term, consider the $a/h \to \infty$ limit of the twisting equation (4) for the through crack case. From (42), (44) and (20b) we obtain

$$\frac{-\sqrt{10}}{24(1+\nu)}\left(g_2(x_2)+\frac{\mathrm{d}g_3(x_2)}{\mathrm{d}x_2}\right)=-\frac{\sigma_2}{6E}, \quad -a \ll x_2 \ll a. \tag{46}$$

This equation is similar to the plate equation from Reissner (1947), introducing transverse shear deformation into the relation between twisting rotation g_2 (or β_2) and transverse displacement g_3 (or w), as follows:

$$\beta_2+\frac{\partial w}{\partial y}=\frac{V_y}{E}\frac{12(1+\nu)}{5}=\theta_2, \tag{47}$$

where θ_2 is the transverse shear deformation.

One could perhaps conclude that the reason why the Reissner formulation does not work is because θ_2 for the infinitely thin plate is not zero. Recall that θ_2 equals zero in the classical plate theory which results from the assumption of infinite shear rigidity. However, this conclusion cannot be valid because the left-hand side of the relation (46) would put a restriction on g_2 and g_3 which is not there in the plane edge crack problem. To illustrate this point for $h/a \to 0$, and by referring to Fig. 2, consider the example of in-plane shear loading ($N_{12} \neq 0$) where the in-plane displacement $g_1 \neq 0$ ($\delta_1 \neq 0$) and the transverse displacement g_3 become zero due to symmetry ($\delta_3 = 0$). The problem should be thought of as a plate theory representation of an antiplane shear elasticity problem. The condition $\theta_2 = 0$ would require that the rotation $g_2 = 0$ ($\delta_2 = 0$). This is obviously incorrect considering the physics of the problem shown in Fig. 2, where $\delta_2 \neq 0$. The coupling of the line spring relations (27) and (28) predicts that both g_1 and g_2 be non-zero, which is the physically expected result for both in-plane shear loading and for twisting loading. Therefore, $\theta_2 \neq 0$ is not the reason why this formulation does not work. This raises the point made by Desvaux (1985) concerning the uncoupling of these equations by setting γ_{12} and γ_{21} to zero in (29a, b). This would clearly lead to the above contradiction. Results obtained by using this assumption for in-plane shear and for twisting loading appear to recover the plane strain result too easily, i.e., for a/h not very large.

The problem is actually that the transverse shear deformation θ_2 of the plate does not become infinite for $h/a \to 0$. If this were the case, then the infinitely thin plate would have no resistance to twisting and the model would work. The transverse shear deformation that is predicted by the Reissner plate theory for twisting of an infinitely thin plate is of order one magnitude. This same plate theory for mode I loading predicts θ_1 to be of order $(a/h)^{1/2}$ for $h/a \to 0$ (see Joseph and Erdogan, 1990). This raises the question of what the elasticity solution of a thin "plate" would predict for twisting resistance. If the answer is, "no resistance", then the Reissner plate theory is not sufficiently advanced to formulate this problem. If the Reissner plate theory prediction is correct, then a more advanced plate theory will still not work with the antisymmetric version of the line spring model (without some adjustment). Regardless of what the elasticity solution is, we can conclude that the Reissner plate theory in twisting is too rigid for the line spring model to work. Therefore an adjustment is necessary.

In order to make this plate theory compatible with the line spring formulation, it is necessary to artificially change the twisting equation (32). Any non-zero stiffness for $h/a \to 0$ must somehow be removed. The only non-zero term results from the twisting kernel, k_{22}, and is given by (42). The derivative term (44), which comes from the kernel k_{23}, approaches zero on its own due to the behavior of the transverse displacement g_3, which is at most a constant for $h/a \to 0$ (note that all displacement quantities must become constant under plane strain conditions by definition). Therefore the equations must be adjusted so that for small h/a the term (42) is subtracted out. The simplest way to achieve this is to subtract the delta function behavior of the kernel from the kernel itself for all h/a. The integral term resulting from k_{22}, i.e.,

$$\frac{1}{2\pi}\int_{-a}^{a} k_{22}(z)g_2(t_2)\,dt_2, \tag{48}$$

is therefore replaced with

$$\frac{1}{2\pi}\int_{-a}^{a}\left(k_{22}(z)+\frac{\sqrt{10}\pi}{12(1+\nu)}\delta(x_2-t_2)\right)g_2(t_2)\,dt_2 = \frac{1}{2\pi}\int_{-a}^{a} k_{22}(z)g_2(t_2)\,dt_2+\frac{\sqrt{10}}{24(1+\nu)}g_2(x_2). \tag{49}$$

After making this adjustment, all integrated terms vanish for $a/h \to \infty$ and the plane strain solution will be recovered as in the mode I case. The modified set of integral equations includes (31) and (33) and is completed by replacing (32) with

$$\frac{h}{24\pi}\int_{-a}^{a}\frac{g_2(t_2)}{(t_2-x_2)^2}\,dt_2+\frac{1}{2\pi}\int_{-a}^{a}\sum_{j=2}^{3}k_{2j}(z)g_j(t_2)\,dt+\frac{\sqrt{10}}{24(1+\nu)}g_2(x_2) - \frac{1}{6\pi h(1+\nu)}\left(\gamma_{21}(x_2)g_1(x_2)+\frac{h}{6}\gamma_{22}(x_2)g_2(x_2)\right)=\frac{1}{Eh^2}F_{20}(x_2), \quad -a<x_2<a. \tag{50}$$

It should be noted that there are other ways of forcing the solution to behave properly at $a/h \to \infty$. For example, the term coming from the kernel k_{23} given by (44) could also be subtracted from the twisting equation so that in effect the transverse shear term (46) would be removed from the equations at $h/a \to 0$. We choose not to remove it because this part of the transverse shear term approaches zero as h/a approaches zero. Another possibility would be to subtract the term given by (42) with $g_2(x_2)$ replaced by $g_2^{\infty}(x_2)$ or $g_2^{\infty}(0)$, where g_2^{∞} would come from the solution of (45a, b). The solution of (45a, b) would represent the plate theory version of the plane edge crack problem. This is not done because it would mean that the plate theory (when used with the line spring model) only has a problem for small h/a. We believe that this same problem exists for all h/a. Therefore, considering the behavior of k_{22} and k_{23}, the chosen method is believed to be reasonable, and as will be seen from the results, does a good job of matching up against existing solutions.

3. SHAPE FUNCTIONS FOR STRESS INTENSITY FACTORS

The stress intensity factor shape functions f_1, f_2 and f_3 that appear in (19) may be obtained by solving the antiplane shear and the plane strain elasticity problems for a strip containing an edge crack of length L and subjected to antisymmetric loading conditions shown in Fig. 2. For an infinite plate with an edge crack the solution for the antiplane shear problem giving mode III deformations around the crack tip is known in closed form (Erdogan, 1978). By referring to Fig. 2 and observing that in this problem σ_{12} is independent of x_2, for a crack surface traction

$$\sigma_{12}(0, x_3) = -G_2(t), \quad t = h/2 - x_3, \quad 0 < t < L, \tag{51}$$

the stress intensity factor may be expressed as (Erdogan, 1978; Joseph and Erdogan, 1987):

$$k_3 = \frac{L}{h}\sqrt{\frac{h}{2\pi}\tan\frac{L}{2h}}\int_{-1}^{1}\frac{G_2(Ls)\sqrt{1-\sin^2\left(\frac{\pi L}{2h}s\right)\Big/\sin^2\left(\frac{\pi L}{2h}\right)}}{\sin\left(\frac{\pi L}{2h}\right)(s-1)}\,ds. \tag{52}$$

For example, if the plane is under in-plane shear loading N_{12} (Fig. 2) then

$$\sigma_{12}(0, x_3) = -G_2(t) = \frac{N_{12}}{h} = \frac{F_1}{h} = \sigma_1 \tag{53}$$

and from (52) we obtain

$$k_3 = \sigma_1\sqrt{h}\sqrt{\xi}\sqrt{\frac{2}{\pi\xi}\tan\left(\frac{\pi\xi}{2}\right)}, \quad \xi = L/h. \tag{54}$$

If, on the other hand, the plate is subjected to uniform twisting moment M_{12} (Fig. 2) we have

$$\sigma_{12}(0, x_3) = -G_2(t) = \frac{6M_{12}}{h^2}\frac{x_3}{h/2} = \frac{6F_2}{h^2}\frac{x_3}{h/2} = \sigma_2\left(1 - \frac{t}{h/2}\right), \tag{55}$$

$$k_3 = \sigma_2\sqrt{h}f_2(\xi) = \sigma_2\sqrt{h}\sqrt{\frac{2}{\pi}\tan\left(\frac{\pi\xi}{2}\right)}\left\{1 - \frac{8}{\pi^2}\int_0^1 \frac{\sin^{-1}\left(t\sin\frac{\pi L}{2h}\right)}{\sqrt{1-t^2}}\,dt\right\}. \tag{56}$$

From (19b), (25) and (54) it may be seen that

$$f_1(\xi) = \sqrt{\frac{2}{\pi}\tan\left(\frac{\pi\xi}{2}\right)}, \quad \alpha_{11} = \frac{-4}{\pi^2}\log\left(\cos\frac{\pi\xi}{2}\right). \tag{57}$$

For the transverse shear loading of the plate (Fig. 2), the problem is a mode II edge crack problem and can be formulated in a straightforward manner (Joseph and Erdogan, 1987). Consider the cracked medium $-\infty < x_1 < \infty$, $(-h/2) < x_3 < (h/2)$ shown in Fig. 2 which is under plane strain conditions. Let $\sigma_{13}(0, x_3)$ acting on the crack surfaces be the only external load. Defining

$$u_3(0, x_3) = w(t), \quad \sigma_{13}(0, x_3) = -G_3(t), \quad t = h/2 - x_3, \quad 0 < t < h, \tag{58}$$

the integral equation for the mode II crack problem may be expressed as (Joseph and Erdogan, 1987; Kaya and Erdogan, 1987):

$$\int_0^L \left\{ \frac{1}{(\tau-t)^2} - \frac{1}{(\tau+t)^2} + \frac{12t\tau}{(\tau+t)^4} - \frac{1}{(2h-t-\tau)^2} + \frac{12(h-t)(h-\tau)}{(2h-t-\tau)^4} + m(t,\tau) \right\} w(\tau)\,d\tau = \frac{-\pi(1+\kappa)}{4\mu} G_3(t), \quad 0 < t < L, \tag{59}$$

where

$$m(t,\tau) = \pi \int_0^\infty [S_1(t,\tau,\alpha) + S_1(h-t,h-\tau,\alpha) + S_2(t,\tau,\alpha) + S_2(h-t,h-\tau,\alpha)]\,d\alpha, \tag{60}$$

$$S_1(t,\tau,\alpha) = \frac{e^{-(\tau+t)\alpha}}{\Delta(\alpha)} \{e^{-2\alpha h}[-2\alpha^3 t\tau + \alpha^2(\tau+t) - \alpha] + 8\alpha^5 h^2 t\tau - 4\alpha^4 h^2(t+\tau) + \alpha^3[2ht + 2h^2 + 2t\tau + 2h\tau] - \alpha^2[t+\tau+2h] + \alpha\}, \tag{61}$$

$$S_2(t,\tau,\alpha) = \frac{\alpha e^{(\tau-t)\alpha}}{\Delta(\alpha)} \{e^{-2\alpha h}[\alpha(\tau-t)+1] + \alpha^3[4h^2 t - 4ht\tau] + \alpha^2[-2h^2 - 2ht + 2h\tau] + \alpha[-\tau + t + 2h] - 1\}, \tag{62}$$

$$\Delta(\alpha) = e^{2\alpha h} - (4\alpha^2 h^2 + 2) + e^{-2\alpha h}. \tag{63}$$

The integral equation (59) is solved by using the technique described by Kaya and Erdogan (1987). Note that in the Reissner theory used to formulate the plate problem, the transverse shear stress σ_{13} is parabolic in x_3. In calculating the mode II stress intensity factor shape function f_3 defined by (19), therefore, the input function G_3 in (59) is assumed to be parabolic with amplitude $\sigma_3 = 3V_1/2$. In tabulating the results, the stress intensity factor for a uniformly distributed crack surface traction is also given. The integral equation (59) is thus solved for

$$\sigma_{13}(0,x_3) = -G_3(t) = -\sigma_3 t(h-t)(2/h)^2, \quad \sigma_3 = \frac{3V_1}{2}, \quad t = h/2 - x_3, \tag{64}$$

$$\sigma_{13}(0,x_3) = -G_3(t) = -\sigma_0. \tag{65}$$

The solution of (59) is of the form (Kaya and Erdogan, 1987):

$$w(t) = \sqrt{L-t}F(t), \quad 0 < t < L \tag{66}$$

where $F(t)$ is a bounded function. After solving the integral equation, the stress intensity factor is obtained from

$$k_2 = \lim_{t \to L} \frac{4\mu}{1+\kappa} \frac{w(t)}{\sqrt{2(L-t)}}. \tag{67}$$

The mode II and III stress intensity factors calculated from (54), (56) and (59) and

Table 1. Normalized mode II and III stress intensity factors for an edge crack in an infinite strip under plane strain and antiplane shear loading conditions [see eqns (53), (55), (64) and (65)]

$\xi = L/h$	$\frac{k_3}{\sigma_1\sqrt{L}}$	$\frac{k_3}{\sigma_2\sqrt{L}}$	$\frac{k_2}{\sigma_3\sqrt{L}}$	$\frac{k_2}{\sigma_0\sqrt{L}}$
→0	1.0	1.0	0.0	1.1215
0.025	1.0003	0.9684	0.0670	1.1215
0.05	1.0010	0.9373	0.1313	1.12155
0.1	1.0041	0.8765	0.2522	1.1219
0.15	1.0094	0.8172	0.3628	1.1233
0.2	1.0170	0.7594	0.4638	1.1264
0.25	1.0270	0.7030	0.5556	1.1323
0.3	1.0398	0.6477	0.6392	1.1419
0.35	1.0558	0.5935	0.7156	1.1562
0.4	1.0753	0.5403	0.7859	1.1763
0.45	1.0992	0.4881	0.8512	1.2034
0.5	1.1284	0.4368	0.9131	1.2391
0.55	1.1642	0.3864	0.9733	1.2854
0.6	1.2085	0.3369	1.0339	1.3450
0.65	1.2642	0.2883	1.0980	1.4221
0.7	1.3360	0.2408	1.1700	1.5229
0.725	1.3801	0.2174	1.2111	1.5852
0.75	1.4315	0.1943	1.2572	1.6578
0.775	1.4922	0.1715	1.3102	1.7435
0.8	1.5650	0.1491	1.3726	1.8459
0.825	1.6541	0.1272	1.4482	1.9708
0.85	1.7663	0.1057	1.5429	2.1269
0.875	1.9125	0.0848	1.6664	2.3289
0.9	2.1133	0.0646	1.8368	2.6037
0.91	2.2171	0.0567	1.9251	2.7448
0.92	2.3404	0.0490	2.0304	2.9116
0.925	2.4114	0.0453	2.0911	3.0074
0.93	2.4901	0.0416	2.1584	3.1132
0.94	2.6767	0.0343	2.3185	3.3634
0.95	2.9180	0.0273	2.5260	3.6854

normalized with respect to $\sigma_i\sqrt{L}$ $(i = 1, 2, 3, 0)$ are shown in Table 1. The results are accurate to within four significant digits. In applying the results to the line spring model, analytical expressions for the shape functions $f_i(\xi)$ $(i = 1, 2, 3)$, $\xi = L/h$, are determined by standard curve fitting, where $f_i(\xi)/\sqrt{\xi}$ correspond to the normalized stress intensity factors given in Table 1. To improve the effectiveness of the fit and to reduce the number of unknown coefficients, it is necessary to take into account the asymptotic form of the stress intensity factors k_2 and k_3 as $L \to 0$ and $L \to h$ or as $\xi \to 0$ and $\xi \to 1$, namely

$$(k_2, k_3) \sim \begin{cases} \sqrt{\xi}, & \xi \to 0, \\ \dfrac{1}{\sqrt{1-\xi}}, & \xi \to 1. \end{cases} \tag{68}$$

Thus, the shape functions f_i $(i = 1, 2, 3)$ defined by (19) and f_0 defined by $k_2 = \sigma_0\sqrt{h}f_0(\xi)$ for the uniform transverse shear stress may be expressed as

$$f_i(\xi) = \frac{\sqrt{\xi}}{\sqrt{1-\xi}} \sum_{j=0}^{8} C_{ij}\xi^j \quad (i = 0, 1, 2, 3), \quad \xi = L/h. \tag{69}$$

The coefficients C_{ij} are given by Table 2.

Table 2. Coefficients C_{ij} for the stress intensity factor shape functions f_i defined by (19) and (69) [Note that $f_i/\sqrt{\xi} = \Sigma C_{ij}\xi^j/(1-\xi)^{1/2} = k_i/(\sigma_i\sqrt{L})$, where $\xi = L/h$ and $k_i/(\sigma_i\sqrt{L})$ are given in Table 1]

j	C_{1j}	C_{2j}	C_{3j}	C_{0j}
0	1.0	1.0	0.0	1.12152
1	−0.5	−1.773760	2.73069	−0.55939
2	0.2861637	0.937496	−3.44019	−0.18069
3	−0.2668382	−0.602894	0.33305	0.39478
4	0.2215318	1.176914	2.80514	2.07787
5	−0.1772160	−2.183231	−2.94406	−5.40893
6	0.1090614	2.906943	0.74775	5.82745
7	−0.0441431	−2.121964	0.63860	−3.11784
8	0.0080606	0.659759	−0.32028	0.67088

4. RESULTS AND DISCUSSION

The system of integral equations, either the "original" equations, (31)–(33), or the "modified" equations, (31), (50) and (33), are solved for the following three loading conditions:

$$F_{10}(x_2) = -N_{12}^{\infty}, \quad F_{20}(x_2) = 0, \quad F_{30}(x_2) = 0, \tag{70}$$

$$F_{20}(x_2) = -M_{12}^{\infty}, \quad F_{10}(x_2) = 0, \quad F_{30}(x_2) = 0, \tag{71}$$

$$F_{30}(x_2) = -V_1^{\infty}, \quad F_{10}(x_2) = 0, \quad F_{20}(x_2) = 0. \tag{72}$$

Equations (70), (71) and (72), respectively, correspond to uniform in-plane shear, twisting, and transverse shear loading of the plate containing a surface crack (Fig. 1). Since the integral equations are coupled, for each loading there will be a primary and a secondary stress intensity factor which are determined from (29) and (19). It should again be emphasized that in the case of transverse shear loading (72) leading to a primarily mode II deformation state around the crack front both in the plane strain problem discussed in the previous section [see eqn (64)] and in the plate problem having a surface crack, σ_{13} is assumed to be parabolic in x_3. For each loading both stress intensity factors are normalized with respect to a primary stress intensity factor obtained from the corresponding two-dimensional elasticity solution of the edge crack problem described in the previous section and given in Table 1. Specifically, the normalizing stress intensity factors for the loading conditions (70), (71) and (72) respectively, are

$$k_{3I} = \sigma_1^{\infty}\sqrt{h}f_1(\xi_0), \quad \xi_0 = L_0/h, \tag{73}$$

$$k_{3T} = \sigma_2^{\infty}\sqrt{h}f_2(\xi_0), \quad \xi_0 = L_0/h, \tag{74}$$

$$k_{2O} = \sigma_3^{\infty}\sqrt{h}f_3(\xi_0), \quad \xi_0 = L_0/h. \tag{75}$$

The functions f_i $(i = 1, 2, 3)$ are given by (69), and $f_i(\xi)/\sqrt{\xi}$ by the first three columns of Table 1, where

$$\sigma_1^{\infty} = \frac{1}{h}N_{12}^{\infty}, \quad \sigma_2^{\infty} = \frac{6}{h^2}M_{12}^{\infty}, \quad \sigma_3^{\infty} = \frac{3}{2h}V_1^{\infty}. \tag{76a–c}$$

The stress intensity factors $k_2(x_2)$ and $k_3(x_2)$ are then transformed into the plane normal to the crack front by using (34) to obtain $k_2'(x_2)$ and $k_3'(x_2)$.

Table 3. Normalized stress intensity factor at the center of a semi-elliptical surface crack in a plate subjected to membrane or in-plane shear, twisting moment and transverse shear [original equations (31)–(33) were used; $\nu = 0.3$]

	a/h									
L_0/h	0.5	1	1.5	2	3	4	5	6	8	10
In-plane shear, mode III, k_3/k_{3I}										
0.05	0.969	0.978	0.981	0.982	0.983	0.983	0.983	0.984	0.984	0.984
0.1	0.899	0.927	0.935	0.939	0.942	0.943	0.943	0.943	0.944	0.944
0.2	0.738	0.800	0.820	0.829	0.837	0.840	0.842	0.843	0.843	0.844
0.3	0.619	0.698	0.727	0.740	0.752	0.758	0.760	0.762	0.764	0.765
0.4	0.547	0.635	0.670	0.688	0.704	0.712	0.716	0.719	0.722	0.724
0.5	0.503	0.600	0.642	0.665	0.688	0.699	0.706	0.710	0.716	0.719
0.6	0.467	0.577	0.629	0.659	0.692	0.709	0.720	0.727	0.736	0.741
0.7	0.420	0.547	0.613	0.653	0.700	0.726	0.743	0.755	0.770	0.780
0.8	0.350	0.489	0.570	0.623	0.688	0.728	0.754	0.773	0.799	0.815
0.85	0.304	0.443	0.529	0.588	0.664	0.711	0.744	0.767	0.800	0.821
0.9	0.249	0.382	0.470	0.532	0.617	0.672	0.711	0.740	0.781	0.809
0.95	0.184	0.299	0.380	0.442	0.530	0.590	0.635	0.670	0.721	0.757
Twisting, mode III, k_3/k_{3T}										
0.05	0.969	0.978	0.981	0.982	0.983	0.983	0.983	0.983	0.983	0.983
0.1	0.895	0.924	0.932	0.936	0.939	0.940	0.940	0.941	0.941	0.941
0.2	0.712	0.779	0.801	0.811	0.819	0.822	0.823	0.824	0.825	0.826
0.3	0.550	0.642	0.674	0.689	0.702	0.708	0.710	0.712	0.714	0.715
0.4	0.411	0.523	0.566	0.587	0.606	0.615	0.619	0.622	0.626	0.628
0.5	0.273	0.410	0.467	0.497	0.526	0.539	0.547	0.552	0.559	0.562
0.6	0.103	0.277	0.357	0.401	0.447	0.470	0.484	0.493	0.504	0.511
0.7	−0.152	0.074	0.193	0.263	0.341	0.382	0.408	0.425	0.447	0.460
0.8	−0.636	−0.335	−0.144	−0.020	0.128	0.211	0.264	0.300	0.347	0.377
0.85	−1.13	−0.766	−0.508	−0.330	−0.109	0.020	0.103	0.162	0.238	0.286
0.9	−2.17	−1.71	−1.32	−1.03	−0.654	−0.425	−0.273	−0.165	−0.021	0.071
0.95	−6.01	−5.27	−4.43	−3.75	−2.81	−2.21	−1.79	−1.49	−1.09	−0.823
Out-of-plane shear, mode II, k_2/k_{2O}										
0.05	1.000	1.000	1.000	1.000	1.000	1.000	1.000	1.000	1.000	1.000
0.1	0.999	1.000	1.000	1.000	1.000	1.000	1.000	1.000	1.000	1.000
0.2	0.988	0.996	0.998	0.999	0.999	1.000	1.000	1.000	1.000	1.000
0.3	0.952	0.982	0.991	0.995	0.998	0.999	0.999	0.999	1.000	1.000
0.4	0.883	0.953	0.976	0.986	0.994	0.997	0.998	0.999	0.999	1.000
0.5	0.790	0.909	0.952	0.972	0.987	0.993	0.996	0.997	0.998	0.999
0.6	0.685	0.851	0.918	0.950	0.978	0.988	0.992	0.995	0.997	0.998
0.7	0.576	0.780	0.873	0.920	0.963	0.979	0.987	0.991	0.995	0.997
0.8	0.467	0.693	0.811	0.876	0.938	0.965	0.978	0.985	0.992	0.995
0.85	0.410	0.640	0.769	0.844	0.919	0.952	0.969	0.979	0.988	0.993
0.9	0.350	0.576	0.714	0.799	0.889	0.932	0.954	0.968	0.982	0.998
0.95	0.277	0.487	0.629	0.723	0.832	0.889	0.921	0.942	0.965	0.977

The effect of the delta function term coming from the twisting kernel (42) is shown in Tables 3 and 4. In these tables a summary of results giving the primary stress intensity factors at the maximum penetration point of a semi-elliptic surface crack corresponding to the loading conditions (70)–(72) is presented. The results are obtained for $\nu = 0.3$ and for the length parameters covering a relatively wide range [$0.05 \leqslant (L_0/h) \leqslant 0.95$ and $0.5 \leqslant a/h \leqslant 10$, Fig. 1]. In Table 3 the original integral equations (31)–(33) are used to obtain the solution. These equations do not predict the plane strain solution for long cracks for either in-plane shear or for twisting loading, as can be seen from the table. Note that the normalized stress intensity factors correspond to the plane edge crack that may be considered as the limiting case of the surface crack for $a \to \infty$, a being the half crack length. Thus the deviation from unity in the primary and from zero in the secondary stress intensity factors should correspond to the effect of the length and profile of the crack. The actual limit predicted by these equations can be obtained from the algebraic solution of (45) together with (29) and (19). Again the plane strain solution, in terms of the plate variables, is simply the solution of these equations without (42), as given by (36a–c). Table 4 is identical

Table 4. Normalized stress intensity factor at the center of a semi-elliptical surface crack in a plate subjected to membrane or in-plane shear, twisting moment and transverse shear [modified equations (31), (50), (33) were used; $\nu = 0.3$]

	a/h									
L_0/h	0.5	1	1.5	2	3	4	5	6	8	10
In-plane shear, mode III, k_3/k_{3t}										
0.05	0.985	0.995	0.997	0.998	0.999	1.000	1.000	1.000	1.000	1.100
0.1	0.948	0.980	0.990	0.994	0.997	0.999	0.999	1.000	1.000	1.000
0.2	0.844	0.932	0.962	0.976	0.988	0.993	0.995	0.997	0.998	0.999
0.3	0.737	0.869	0.921	0.946	0.970	0.980	0.986	0.989	0.993	0.995
0.4	0.643	0.799	0.868	0.905	0.942	0.959	0.969	0.975	0.982	0.986
0.5	0.559	0.723	0.805	0.853	0.903	0.928	0.944	0.954	0.966	0.973
0.6	0.479	0.642	0.732	0.787	0.851	0.886	0.908	0.923	0.941	0.953
0.7	0.398	0.552	0.646	0.709	0.785	0.830	0.859	0.880	0.907	0.924
0.8	0.310	0.452	0.546	0.613	0.701	0.756	0.794	0.821	0.858	0.882
0.85	0.264	0.396	0.489	0.557	0.649	0.709	0.751	0.782	0.825	0.853
0.9	0.214	0.334	0.423	0.490	0.586	0.650	0.696	0.731	0.779	0.813
0.95	0.158	0.260	0.340	0.404	0.498	0.565	0.614	0.652	0.707	0.746
Twisting, mode III, k_3/k_{3T}										
0.05	0.985	0.995	0.997	0.998	0.999	1.000	1.000	1.000	1.000	1.000
0.1	0.946	0.980	0.990	0.994	0.997	0.999	0.999	1.000	1.000	1.000
0.2	0.832	0.928	0.960	0.975	0.988	0.993	0.995	0.997	0.998	0.999
0.3	0.696	0.852	0.912	0.941	0.968	0.979	0.985	0.988	0.992	0.994
0.4	0.547	0.753	0.841	0.888	0.933	0.953	0.965	0.972	0.980	0.984
0.5	0.369	0.617	0.738	0.805	0.875	0.909	0.929	0.942	0.957	0.966
0.6	0.132	0.419	0.577	0.672	0.777	0.832	0.866	0.888	0.916	0.932
0.7	−0.234	0.091	0.299	0.436	0.599	0.690	0.747	0.787	0.837	0.868
0.8	−0.942	−0.588	−0.297	−0.083	0.196	0.364	0.475	0.552	0.653	0.716
0.85	−1.67	−1.32	−0.954	−0.664	−0.262	−0.011	0.159	0.279	0.437	0.537
0.9	−3.26	−2.95	−2.45	−2.00	−1.34	−0.897	−0.592	−0.374	−0.081	0.106
0.95	−9.18	−9.22	−8.30	−7.31	−5.68	−4.52	−3.69	−3.08	−2.25	−1.71
Out-of-plane shear, mode II, k_2/k_{2t}										
0.05	1.000	1.000	1.000	1.000	1.000	1.000	1.000	1.000	1.000	1.000
0.1	0.999	1.000	1.000	1.000	1.000	1.000	1.000	1.000	1.000	1.000
0.2	0.988	0.996	0.988	0.999	0.999	1.000	1.000	1.000	1.000	1.000
0.3	0.952	0.982	0.991	0.995	0.998	0.999	0.999	0.999	1.000	1.000
0.4	0.883	0.954	0.977	0.986	0.994	0.997	0.998	0.999	0.999	1.000
0.5	0.790	0.910	0.953	0.973	0.988	0.994	0.996	0.998	0.999	0.999
0.6	0.685	0.852	0.920	0.952	0.979	0.989	0.994	0.996	0.998	0.999
0.7	0.576	0.781	0.875	0.923	0.966	0.982	0.990	0.994	0.997	0.998
0.8	0.467	0.694	0.814	0.880	0.944	0.970	0.982	0.988	0.994	0.997
0.85	0.411	0.642	0.773	0.849	0.926	0.959	0.975	0.984	0.992	0.995
0.9	0.350	0.578	0.718	0.805	0.897	0.940	0.962	0.974	0.987	0.992
0.95	0.278	0.488	0.633	0.730	0.842	0.899	0.932	0.951	0.972	0.983

to Table 3 except that the modified equations (31), (50) and (33), which include the delta function behavior of the twisting kernel, are used to obtain the solution. As a/h gets large for a given crack depth L_0/h, the plane strain solution is approached in Table 4 for all loading cases.

Some sample results showing the effect of crack front curvature on the stress intensity factors are shown in Fig. 3 for an infinite plate containing a semi-elliptic surface crack and subjected to in-plane shear loading N_{12}^{∞} away from the crack region. Results for this figure were obtained with the original integral equations, (31)–(33). Note that because of the crack front curvature the difference between particularly the secondary stress intensity factors k_2 and k_2' is quite large. All the remaining results in the paper are given in terms of k_2' and k_3', which are referred to the coordinate system x_1', x_2', x_3' where x_2' is a tangent to the crack front and x_1' is identical to x_1.

For the same in-plane shear problem whose solution is presented in Fig. 3, the mode II and III stress intensity factors obtained by Sorensen and Smith (1977) by using the alternating method and that given by the line spring model are shown in Fig. 4. The original

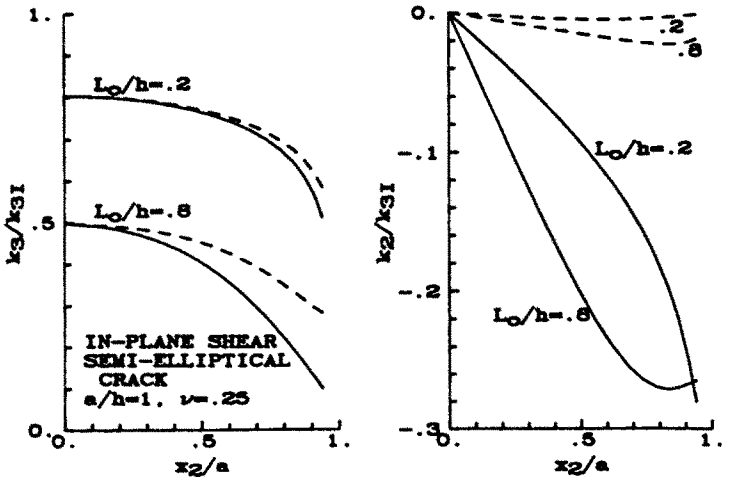

Fig. 3. Comparison of the stress intensity factors k_2' and k_3' obtained from (34) (full lines) with k_2 and k_3, which are defined by (11) and calculated from (19) (dashed lines) for a plate with a semi-elliptical surface crack under in-plane shear loading N_{12}^{∞}. Original equations (31)–(33) were used; $a/h = 1$, $\nu = 0.25$.

integral equations were also used for this example. In Fig. 5 the modified equations are used for the same problem. Similar plots are given in Figs 6 and 7 for $a/h = 2.0$, 0.5, and 4.0. In comparing these results it may be worthwhile to observe that while the line spring results are necessarily approximate, the degree of accuracy of the results obtained from the alternating method is not completely known. The in-plane shear solution of Sorensen and Smith (1977) is reported to be in excellent agreement with the finite element–alternating results obtained by Simon *et al.* (1987). However, Raju and Newman (1979), in comparing the mode I stress intensity factors given by various numerical methods, found that there was a discrepancy of 10–25% between their finite element results and the results obtained by Smith and Sorensen (1974) from the alternating method. On the other hand, for the mode I surface crack problem rather good agreement has been observed between finite element and line spring results (see, for example, Joseph and Erdogan, 1989).

For the case of transverse shear, there are two sources for which a comparison with the present method is possible. Simon *et al.* (1987) and Nikishkov and Atluri (1987), who, by using the "Equivalent Domain Integral" method based on the method of Virtual Crack

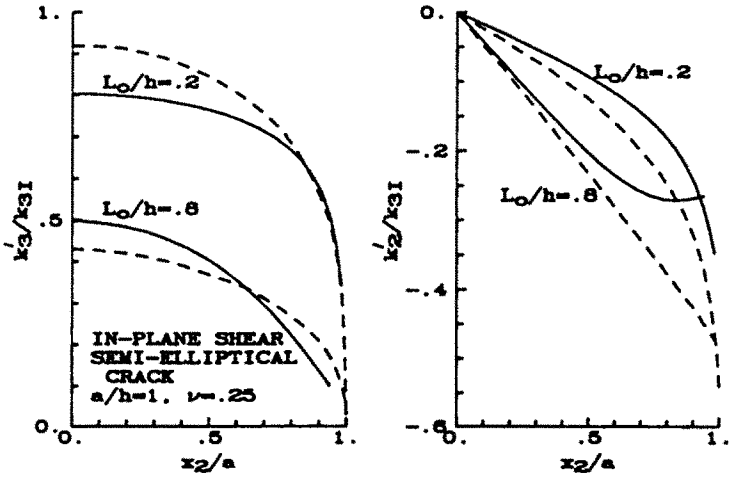

Fig. 4. Comparison of the normalized mode II and III stress intensity factors k_2' and k_3' given by Sorensen and Smith (1977) (dashed lines) and by the line spring model (full lines) for a plate with a semi-elliptical surface crack under in-plane shear loading N_{12}^{∞}. Original equations (31)–(33) were used (see Fig. 5); $a/h = 1$, $\nu = 0.25$.

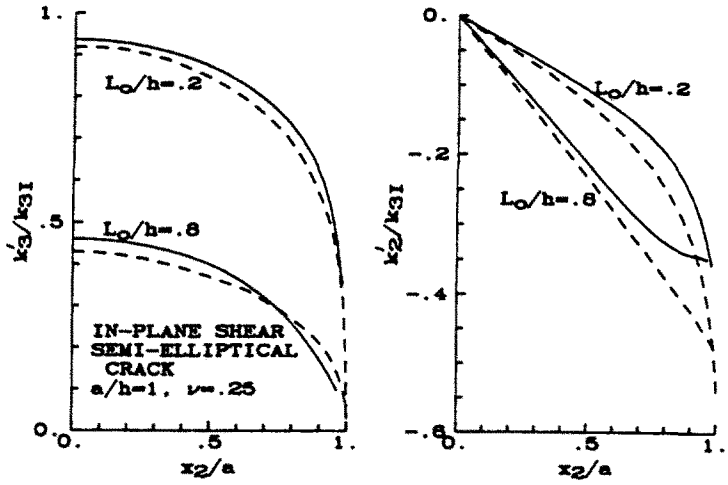

Fig. 5. Comparison of the normalized mode II and III stress intensity factors k_2' and k_3' given by Sorensen and Smith (1977) (dashed lines) and by the line spring model (full lines) for a plate with a semi-elliptical surface crack under in-plane shear loading N_{12}^{∞}. Modified equations (31), (50) and (33) were used; $a/h = 1$, $\nu = 0.25$.

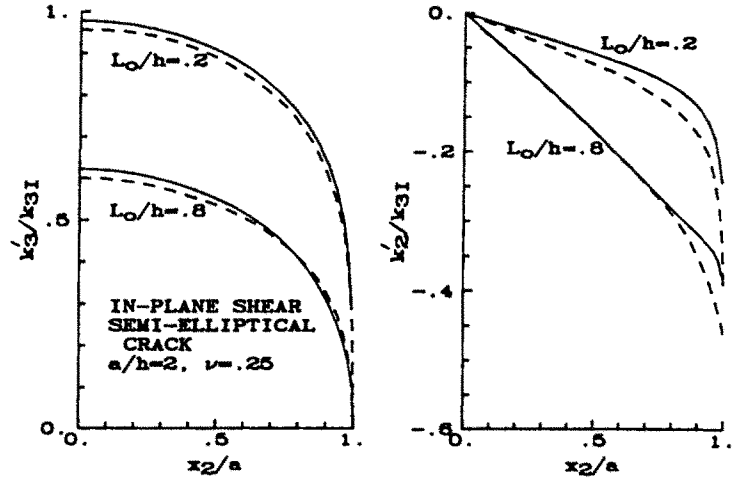

Fig. 6. Comparison of the normalized mode II and III stress intensity factors k_2' and k_3' given by Sorensen and Smith (1977) (dashed lines) and by the line spring model (full lines) for a plate with a semi-elliptical surface crack under in-plane shear loading N_{12}^{∞}. Modified equations (31), (50) and (33) were used; $a/h = 2$, $\nu = 0.25$.

Extension, have investigated the problem of a cantilever square plate (length = 2.5 × thickness) with a transverse surface crack ($a/h = 0.5$, $L_0/h = 0.25$) subjected to transverse end loading. The plate dimensions are such that a comparison to the infinite plate solution presented is acceptable, although some error is expected. The side dimensions of the plate are 2.5 times the total crack length, $2a$. The loading is such that a parabolic shear distribution at the crack location of the uncracked plate is a reasonable assumption (see Simon *et al.*, 1987). Also, for $a/h = 0.5$ the line spring model is near its limit of reasonable application (see Figs 4–6). The results are presented in Fig. 8 for the original equations and in Fig. 9 for the modified equations. The difference between the two line spring solutions for this loading is due to secondary contributions. For in-plane shear and twisting the differences between the two sets of equations result from primary effects and are therefore greater (see Figs 4 and 5). Comparison with the solution of Nikishkov and Atluri (1987) is quite good. The specific method chosen for comparison from Nikishkov and Atluri (1987) is "from displacements" (see Figs 19 and 20 of this reference). It is not known which of the two sets of numerical results is more accurate. The comparison in these figures shows that

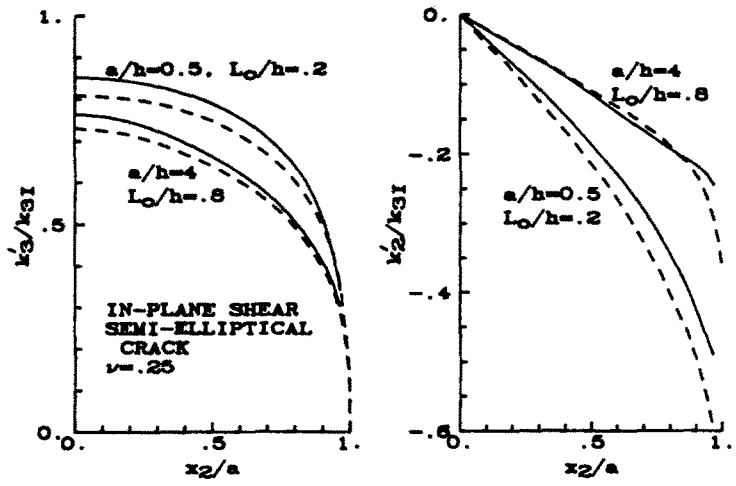

Fig. 7. Comparison of the normalized mode II and III stress intensity factors k'_2 and k'_3 given by Sorensen and Smith (1977) (dashed lines) and by the line spring model (full lines) for a plate with a semi-elliptical surface crack under in-plane shear loading N^{∞}_{12}. Modified equations (31), (50) and (33) were used; $a/h = 0.5$ and 4.0, $\nu = 0.25$.

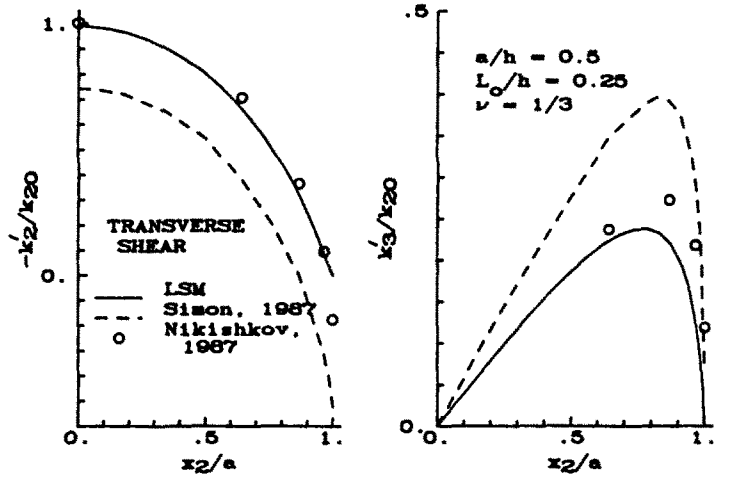

Fig. 8. Comparison of the normalized mode II and III stress intensity factors k'_2 and k'_3 given by Simon *et al.* (1987) and Nikishkov and Atluri (1987) and the line spring model for a plate with a semi-elliptical surface crack under transverse shear loading V^{∞}_1. Original equations (31)–(33) were used (see Fig. 9); $a/h = 0.5$, $\nu = 1/3$.

the line spring model predicts the general trend of the more advanced methods and is also comparable for transverse shear loading. The remaining results that are presented in this paper are from the solution of the modified equations (31), (50) and (33).

Some sample results obtained from (70), (71) and (72) showing the stress intensity factor distribution along the crack front for $a/h = 1$, $\nu = 0.3$ and $L_0/h = 0.1$, 0.3, 0.5, 0.7 and 0.9 are given in Figs 10–15 (see Fig. 1 for notation). Figures 10–12 show the normalized stress intensity factor for a crack with a rectangular profile, namely for $L(x_2) = L_0$, $-a < x_2 < a$ (Fig. 1). The results shown in Figs 13–15 are for a semi-elliptic crack front for which

$$L(x_2) = L_0\sqrt{1-(x_2/a)^2}, \quad -a < x_2 < a. \tag{77}$$

Each figure shows the secondary as well as the primary stress intensity factor. For example, in Fig. 11 the plate containing a rectangular crack is under twisting moment M^{∞}_{12} (Fig. 1). Consequently, k'_3 is the primary and k'_2 is the secondary stress intensity factor. Also note

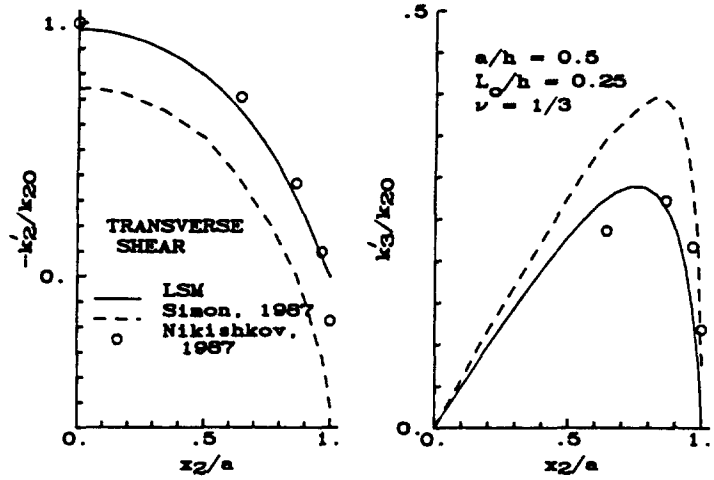

Fig. 9. Comparison of the normalized mode II and III stress intensity factors k'_2 and k'_3 given by Simon *et al.* (1987) and Nikishkov and Atluri (1987) and the line spring model for a plate with a semi-elliptical surface crack under transverse shear loading V_1^∞. Modified equations (31), (50) and (33) were used; $a/h = 0.5$, $\nu = 1/3$.

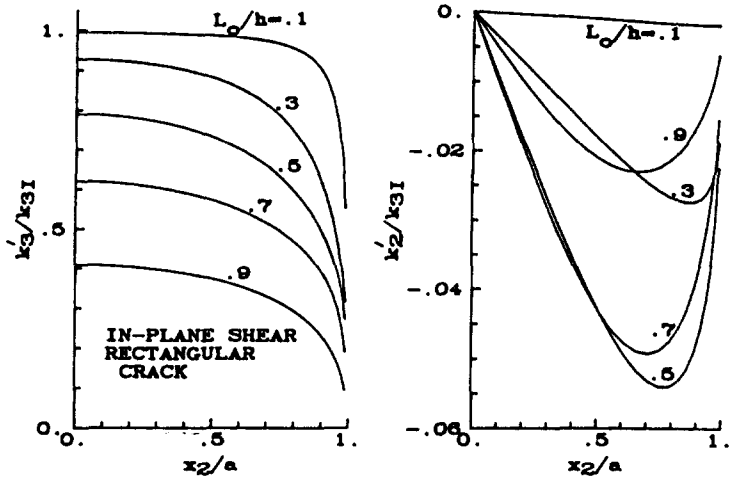

Fig. 10. The variation of normalized mode II and III stress intensity factors along the crack front in a plate containing a rectangular crack of depth L_0 under in-plane shear loading N_{12}^∞. Modified equations (31), (50) and (33) were used; $a/h = 1$, $\nu = 0.3$.

that for the rectangular crack the crack front is parallel to the x_2 axis, $\theta = 0$, and consequently $k'_2 = k_2$ and $k'_3 = k_3$.

The similar problem of a surface crack in shells under mixed mode loading conditions was considered in a recent study by Joseph and Erdogan (1988), where again Reissner's transverse shear theory was used. This formulation needs to be corrected by determining the delta function behavior of the twisting kernel and subtracting it from the equation as was done for this paper. Also (34) must be used to compensate for the crack front curvature. With these two omissions, the results in that paper correspond to the results given by Table 3 and by the dashed lines of Fig. 3 in this paper.

As indicated before, unlike problems of plane elasticity, the stress intensity factors in surface crack problems are dependent on Poisson's ratio, ν. The effect of ν has been studied in mode I problems and has been shown not to be very significant. For the three main antisymmetric loading conditions (70)–(72) the influence of Poisson's ratio on the corresponding primary stress intensity factors is shown in Table 5. In these examples the crack profile is assumed to be semi-elliptic and only the stress intensity factor at the maximum penetration point of the crack is tabulated. Note that at this point for the loading

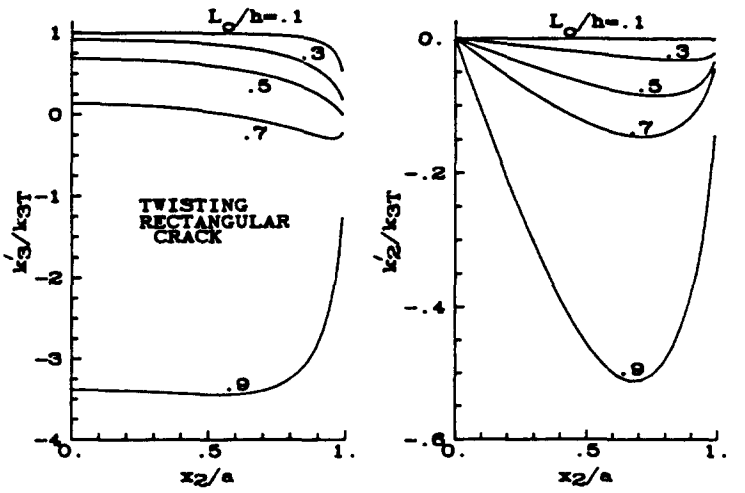

Fig. 11. The variation of normalized mode II and III stress intensity factors along the crack front in a plate containing a rectangular crack of depth L_0 under twisting moment M_{12}^{∞}. Modified equations (31), (50) and (33) were used; $a/h = 1$, $\nu = 0.3$.

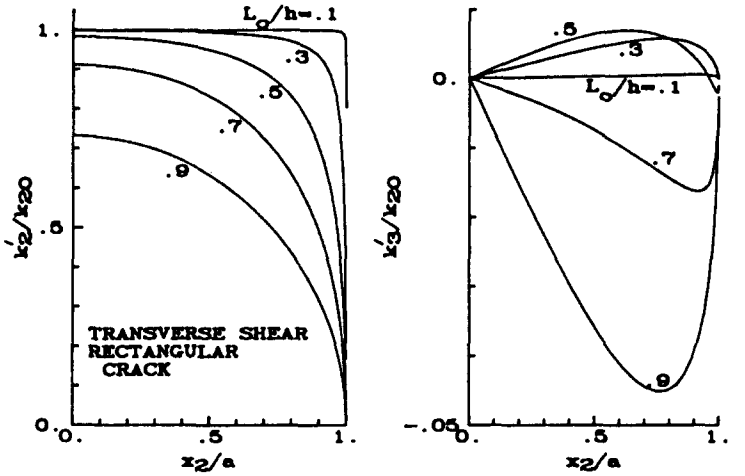

Fig. 12. The variation of normalized mode II and III stress intensity factors along the crack front in a plate containing a rectangular crack of depth L_0 under transverse shear loading V_1^{∞}. Modified equations (31), (50) and (33) were used; $a/h = 1$, $\nu = 0.3$.

conditions considered the secondary stress intensity factors are zero. Even though for very deep cracks under transverse shear loading the effect of ν (varying between 0 and 0.5) on k_2 may be as high as 33%, for the practical values of ν and for most crack geometries the influence of Poisson's ratio is not expected to be significant.

5. CONCLUDING REMARKS

The line spring model, which is known to provide reasonably accurate results for mode I surface crack problems in plates and shells, has been presented for the case of antisymmetric loading conditions. The Reissner plate theory was used to formulate the plate problem. This is the simplest plate theory in which all three of the unknown stress resultants, namely in-plane shear (N_{xy}), twisting (M_{xy}), and transverse shear (V_x), can be prescribed individually on a given boundary. This allows for a systematic development of the model.

In the antisymmetric problem the mode II and III stress intensity factors are coupled and their relative magnitudes along the crack front for a given loading condition depend heavily on the crack front curvature. This requires transformation of the calculated stress intensity factors k_2 and k_3 referred to the x_1, x_2, x_3 coordinate system into k_2' and k_3' which

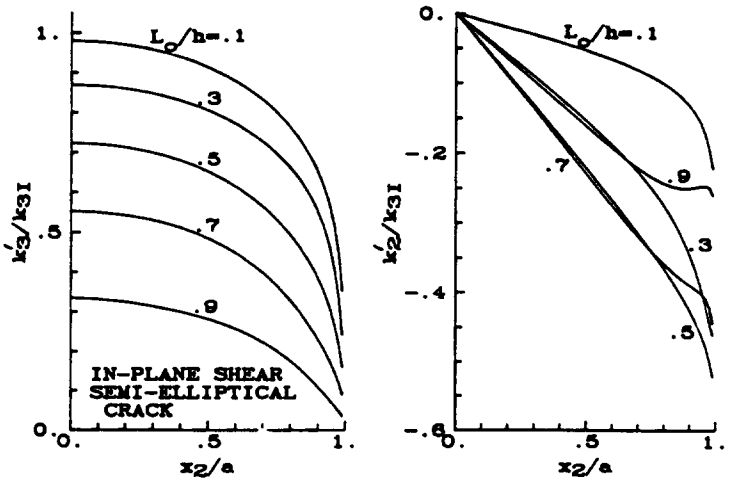

Fig. 13. The variation of normalized mode II and III stress intensity factors along the crack front in a plate containing a semi-elliptic crack of semi-axes a and L_0 under in-plane shear loading N_{12}^{∞}. Modified equations (31), (50) and (33) were used; $a/h = 1$, $\nu = 0.3$.

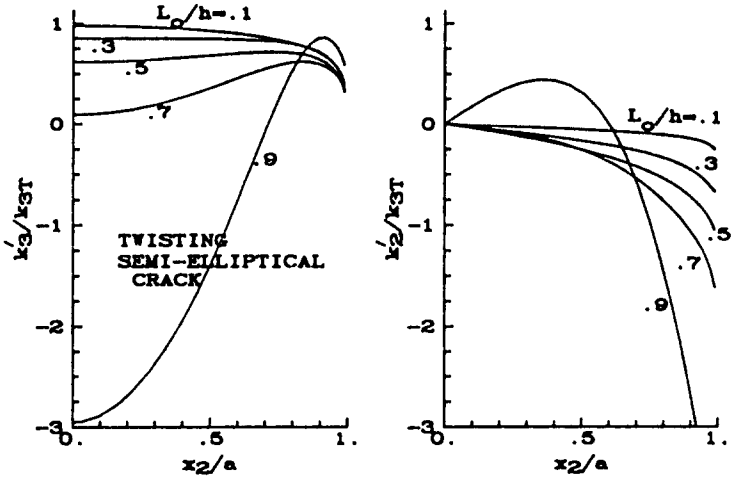

Fig. 14. The variation of normalized mode II and III stress intensity factors along the crack front in a plate containing a semi-elliptic crack of semi-axes a and L_0 under twisting moment M_{12}^{∞}. Modified equations (31), (50) and (33) were used; $a/h = 1$, $\nu = 0.3$.

are referred to x_1', x_2', x_3', where $x_1' = x_1$, x_2' is tangent and x_3' normal to the crack front (Fig. 1).

It was found that the line spring formulation given leads to a result that does not recover the plane strain solution for large crack lengths, a limiting behavior that should be inherent in the model. However, this shortcoming appears to be built into the "plate theory" rather than being a consequence of the line spring approximation. The discrepancy can be removed by subtracting the large a/h behavior of the twisting kernel, k_{22}, from itself for all values of a/h. Therefore as $a/h \to \infty$, the integral term resulting from this kernel goes to zero like all other integral terms in the integral equations and in the limit allows the solution to approach the plane strain solution. The comparison of the results thus obtained with existing numerical solutions is found to be quite good.

Acknowledgements—This work was supported by NSF under Grant MSM-8613611 and by NASA-Langley under Grant NAG-1-713. The authors are grateful to the reviewers for drawing attention to Desvaux's work and for critical and very helpful comments on the original manuscipt.

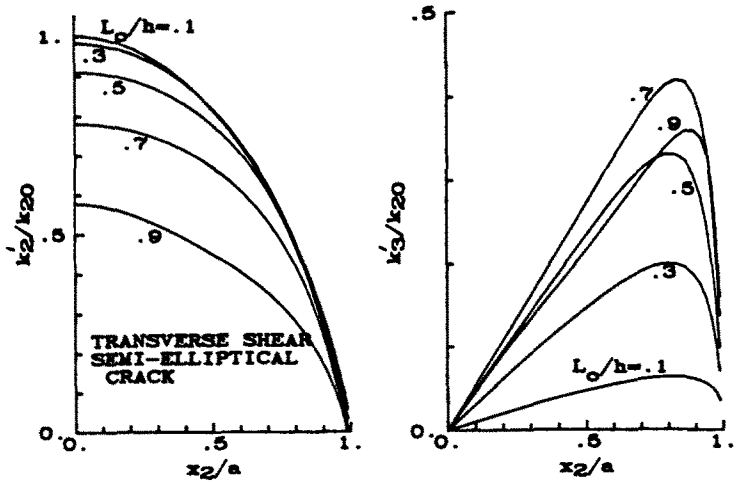

Fig. 15. The variation of normalized mode II and III stress intensity factors along the crack front in a plate containing a semi-elliptic crack of semi-axes a and L_0 under transverse shear loading V_T^*. Modified equations (31), (50) and (33) were used; $a/h = 1$, $\nu = 0.3$.

Table 5. The effect of Poisson's ratio on the normalized stress intensity factor at the center of a semi-elliptical crack subjected to out-of-plane shear, in-plane shear, and twisting loads, $a/h = 1$ [the modified equations (31), (50), (33) were used]

ν	In-plane shear, mode III, $k_{\text{III}}/k_{\text{III}}$			Twisting, mode III, $k_{\text{III}}/k_{\text{III}}$			Out-of-plane shear, mode II, k_2/k_{20}		
L_0/h	0.0	0.3	0.5	0.0	0.3	0.5	0.0	0.3	0.5
0.05	0.997	0.995	0.993	0.997	0.995	0.993	1.00	1.00	1.00
0.1	0.990	0.980	0.974	0.990	0.980	0.973	1.00	1.00	1.00
0.2	0.961	0.932	0.914	0.960	0.928	0.908	0.994	0.996	0.997
0.3	0.917	0.869	0.841	0.909	0.852	0.819	0.974	0.982	0.987
0.4	0.860	0.799	0.764	0.832	0.753	0.707	0.936	0.954	0.966
0.5	0.790	0.723	0.687	0.718	0.617	0.562	0.879	0.910	0.933
0.6	0.708	0.642	0.606	0.539	0.419	0.355	0.807	0.852	0.886
0.7	0.615	0.552	0.519	0.232	0.091	0.018	0.723	0.781	0.828
0.8	0.510	0.452	0.422	−0.420	−0.588	−0.668	0.626	0.694	0.752
0.85	0.451	0.396	0.368	−1.13	−1.32	−1.40	0.570	0.642	0.704
0.9	0.386	0.334	0.308	−2.75	−2.95	−3.03	0.505	0.578	0.644
0.95	0.307	0.260	0.237	−9.03	−9.22	−9.21	0.418	0.488	0.555

REFERENCES

Atluri, S. N. and Nishioka, T. (1986). Computational methods for three-dimensional problems of fracture. In *Computational Methods in the Mechanics of Fracture* (Edited by S. N. Atluri), pp. 229–287. North Holland, Amsterdam.

Desvaux, G. J. (1985). The line spring model for surface flaw, an extension to Mode II and Mode III. Master's thesis, Department of Mechanical Engineering, Massachusetts Institute of Technology.

Erdogan, F. (1978) Mixed boundary-value problems in mechanics. In *Mechanics Today* (Edited by S. Nemat-Nasser), Vol. 4, pp. 1–86. Pergamon Press, Oxford.

Erdogan, F. (1986). The line spring model. In *Computational Methods in the Mechanics of Fracture* (Edited by S. N. Atluri), pp. 289–309. North Holland, Amsterdam.

Joseph, P. F. and Erdogan, F. (July 1987). Plates and shells containing a surface crack under general loading conditions. NASA Contractor Report 178328, NASA Langley Research Center.

Joseph, P. F. and Erdogan, F. (1988). A surface crack in shells under mixed mode loading conditions. *ASME J. Appl. Mech.* 55(4), 795–804.

Joseph, P. F. and Erdogan, F. (1989). Surface crack problems in plates. *Int. J. Fracture* 41, 105–131.

Joseph, P. F. and Erdogan, F. (1990). Bending of a thin Reissner plate with a through crack. *ASME J. Appl. Mech.* (to appear).

Kaya, A. C. and Erdogan, F. (1987). On the solution of integral equations with strongly singular kernels. *Q. Appl. Math.* 45(1), 105–122.

Li, V. C. and Rice, J. R. (1983) Precursory surface deformation in great plate boundary earthquake sequences. *Bull. Seismol. Soc. Am.* 73(5), 1415–1434.

Newman, J. C. Jr. and Raju, I. S. (1986). Stress intensity factor equations for cracks in three-dimensional finite bodies subjected to tension and bending loads. In *Computational Methods in the Mechanics of Fracture* (Edited by S. N. Atluri), pp. 289–309. North Holland, Amsterdam.

Nikishkov, G. P. and Atluri, S. N. (1987). Calculation of fracture mechanics parameters for an arbitrary three-dimensional crack, by the 'Equivalent Domain Integral' method. *Int. J. Numer. Meth. Engng* **24**, 1801–1821.

Raju, I. S. and Newman, J. C. Jr. (1979). Stress intensity factors for a wide range of semi-elliptical surface cracks in finite thickness plates. *Engng Fracture Mech.* **11**, 817–829.

Reissner, E. (1945). The effect of transverse shear deformation on the bending of elastic plates. *ASME J. Appl. Mech.* **12**, A69–A77.

Reissner, E. (1947). On bending of elastic plates. *Q. Appl. Math.* **5**, 55–68.

Rice, J. R. (1972). The line spring model for surface flaws. In *The Surface Crack: Physical Problems and Computational Solutions* (Edited by J. L. Swedlow), pp. 171–186. ASME, New York.

Rice, J. R. and Levy, N. (1972). The part-through surface crack in an elastic plate. *ASME J. Appl. Mech.* **39**, 185–194.

Simon, H. L., O'Donoghue, P. E. and Atluri, S. N. (1987). A finite-element-alternating technique for evaluating mixed mode stress intensity factors for part-through surface flaws. *Int. J. Numer. Meth. Engng* **24**, 689–709.

Smith, F. N. and Sorensen, D. R. (1974). Mixed mode stress intensity factors for semi-elliptical surface cracks. NASA CR-134684.

Sorensen, D. R. and Smith, F. W. (1977). Semielliptical surface cracks subjected to shear loading. *Pressure Vessel Technology—Part II, Third International Conference*, Tokyo, Japan, pp. 545–551. ASME, New York.

Tschegg, E. K., Ritchie, R. O. and McClintock, F. A. (1983). On the influence of rubbing fracture surfaces on fatigue crack propagation in mode III. *Int. J. Fatigue* **5**, 29–35.